Modeling Free Acceleration of a Salient Synchronous Machine Using Two-Axis Theory

Abdullah H. Akca and Lingling Fan, *Senior Member, IEEE*

***Abstract*—This paper investigates a nonlinear simulation model of a synchronous machine derived from space vector. The model is built to show acceleration from zero speed to nominal speed while its stator is connected to a three-phase voltage source. The two-axis modeling approach is adopted to emulate the three-phase stator circuits as *dq* circuits on the rotor. The entire model is based on the rotor reference frame. For swing dynamics, torque/speed dynamic equation is adopted without any approximation. A machine started by a three-phase voltage source at its stator is simulated via MATLAB/Simulink. The simulation results demonstrate how to start a synchronous machine: without excitation voltage and with increased resistance in the excitation circuit.**

***Index Terms*—Space Vector (SV), Synchronous Machine (SM), Magnetomotive Force (MMF), Electromotive Force (EMF), dq fictitious circuit**

I. Introduction

Instead of using Park's transformation, we show in this article that Park's transformation can be viewed to use two fictitious circuits on rotor to represent the three-phase stator circuit. For synchronous generator analysis, this approach is easy to be understood and provides great insights. The key concept here is space vector.

When a standing still three-phase synchronous machine connected to a three-phase voltage source at its stator, three-phase balanced stator currents create rotating magnetomotive force (MMF) (Ampers law) in the air gap. This MMF generates a rotating flux (armature flux) in the air gap. This flux induces sinusoidal EMF in the rotor windings. So a current starts to flow through the rotor circuit which forms a rotating MMF and further a rotor flux. Interaction of the armature flux and rotor flux (stator MMF or rotor MMF) leads to electromagnetic torque and the machine may start rotate. This procedure is same as the induction effect of an induction motor.

The difference of a salient synchronous machine and an induction machine resides in the salience of the synchronous machine rotor. Unlike an induction machine where the rotor is round and the airgap is uniform, a salient synchronous machine has a nonsymmetric rotor and an nonuniform airgap. Modeling of a synchronous machine is easier using two-axis theory. Basically speaking, two-axis theory decomposes MMF into d and q axes, where d-axis is aligned with the rotor flux (generated by the excitation current) direction, q-axis lags d-axis by 90 degree. See Fig. 1. That way, for d-axis MMF, the airgap path is fixed and for q-axis MMF, the airgap path is also fixed. This in turn results in fixed inductances of dq-axis (L_d and L_q). It is also easy to see that L_d should be greater than L_q since the airgap path in d-axis direction is much shorter than that in the q-axis direction.

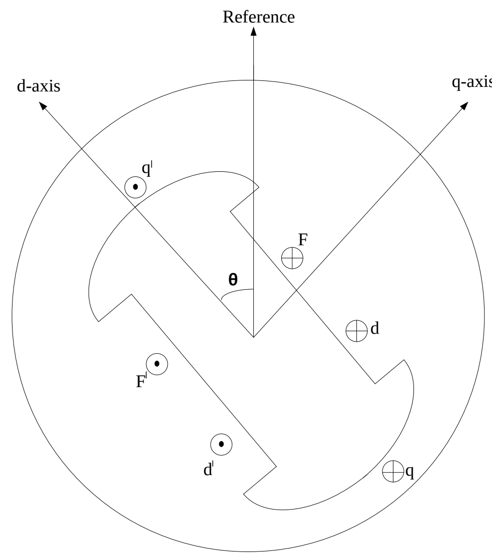

Fig. 1: Synchronous machine dq axes positions, excitation winding FF', and two fictitious windings dd' qq'.

The effect of the three-phase stator circuits on forming an MMF is similar as two fictitious circuits on the rotor on forming a d-axis MMF and a q-axis MMF. Therefore, the two windings dd' and qq' in Fig. 1 are used to represent the stator circuits. To start a synchronous machine, induction effect is key. Therefore, the excitation voltage source is short cut.

In the rest of the paper, Section II presents machine modeling based on space vector concept. Section III presents the simulation model and case study results. Section IV concludes the paper.

II. Space Vector-Based Synchronous Machine Modeling

A. Space vector and Park's transformation

The concept of space vector aligns with the physics of Ampere's Law: three-phase balanced stator currents form a rotating MMF. The rotating speed is the electric frequency. The MMFs due to each phase stator current are expressed as follow.

$$\begin{aligned} f_a(\alpha,t) &= NI_a(t)\cos(\alpha) \\ f_b(\alpha,t) &= NI_b(t)\cos\left(\alpha-\frac{2\pi}{3}\right) \\ f_c(\alpha,t) &= NI_c(t)\cos\left(\alpha+\frac{2\pi}{3}\right) \end{aligned} \tag{1}$$

where N is the number of windings, α is a position in the airgap and the three-phase balanced currents are expressed as follows.

$$\begin{aligned} i_a(t) &= I_m \cos(\omega_s t + \theta_{a0}) \\ i_b(t) &= I_m \cos\left(\omega_s t + \theta_{a0} - \frac{2\pi}{3}\right) \\ i_c(t) &= I_m \cos\left(\omega_s t + \theta_{a0} + \frac{2\pi}{3}\right) \end{aligned} \quad (2)$$

where θ_{a0} is the initial phase angle of the phase-a current.

Therefore the total MMF due to the stator currents is:

$$\begin{aligned} f_s(\alpha) &= N\left(i_a \cos(\alpha) + i_b \cos\left(\alpha - \frac{2\pi}{3}\right) + i_c \cos\left(\alpha + \frac{2\pi}{3}\right)\right) \\ &= 1.5 I_m \cos(\alpha - \theta_a) \end{aligned} \quad (3)$$

Writing it in the form of a space vector to indicate the magnitude and the position of the maximum MMF, we have

$$\overrightarrow{f}_s = 1.5 N I_m e^{j\theta_a} = N i_a + N i_b e^{j2\pi/3} + N i_c e^{-j2\pi/3} \quad (4)$$

It can be found that the space vector of the MMF is proportional to the analytic form of $i_a(t)$. In turn, space vector representation of a variable follows all rules of the original variable.

On zero sequence $i_a = i_b = i_c$, so related space vector value will be zero. This means, there will not be any MMF or torque generation for zero sequence.

From the equations above, space vector notation of the stator MMF for a balanced set can be shown as

$$\overrightarrow{f_s}(t) = \frac{3}{2} N I_a e^{-j(\omega_s t + \theta_0)}. \quad (5)$$

This vector will be decomposed into d-axis and q-axis components aligned with the rotor reference frame. Assume that the rotor rotating speed is ω_m, then we have:

$$f_{sdq} = \frac{3}{2} N I_m e^{-j(\omega_s - \omega_m)t} \quad (6)$$

$$f_{sd} = \frac{3}{2} N I_m \cos(\omega_s - \omega_m)t \quad (7)$$

$$f_{sq} = -\frac{3}{2} N I_m \sin(\omega_s - \omega_m)t \quad (8)$$

The dq-axis MMFs produces dq fluxes in the airgap. The d-axis flux will link with the rotor circuit FF' and generates flux linkage for FF'. Based on Faraday's law, if this flux linkage is varying, FF' will have induced EMF and in turn current i_F. i_F in turn will generate an MMF and flux. Therefore, the total d-axis air gap flux is due to both i_d and i_F while the q-axis flux is due to i_q only.

From the forming of rotating magnetic field, we introduce the space vector definition as:

$$\overrightarrow{i} = \frac{2}{3}(i_a + i_b e^{j2\pi/3} + i_c e^{-j2\pi/3}) \quad (9)$$

$\frac{2}{3}$ is introduced as a scaling factor so that the magnitude of the space vector is the same as that of the per-phase signals.

If we view this space vector from the rotor reference frame as i_{dq}, then

$$\overline{i_{dq}} e^{j(\omega_m t + \theta_0)} = \overrightarrow{i} = I_m e^{j(\omega_s + \theta_{a0})} \quad (10)$$

where θ_0 is the initial rotor angle position. Or

$$\overline{i_{dq}} = e^{-j\theta} \overrightarrow{i} = \frac{2}{3} e^{-j\theta}\left(i_a + i_b e^{j\frac{2\pi}{3}} + i_c e^{-j\frac{2\pi}{3}}\right) \quad (11)$$

where $\theta = \omega_m t + \theta_0$ is the rotor position.

This transformation aligns with the Park's transformation defined in Kraus' book [1], where

$$\begin{bmatrix} i_0 \\ i_d \\ i_q \end{bmatrix} = \frac{2}{3} \begin{bmatrix} \frac{1}{2} & \frac{1}{2} & \frac{1}{2} \\ \cos(\theta) & \cos\left(\theta - \frac{2\pi}{3}\right) & \cos\left(\theta + \frac{2\pi}{3}\right) \\ \sin(\theta) & \sin\left(\theta - \frac{2\pi}{3}\right) & \sin\left(\theta + \frac{2\pi}{3}\right) \end{bmatrix} \begin{bmatrix} i_a \\ i_b \\ i_c \end{bmatrix}$$

If we use the above space vector notation, for three-phase power $p = v_a i_a + v_b i_b + v_c i_c$, assume balanced operation, we will end up with

$$p = \frac{3}{2}(v_d i_d + v_q i_q) \quad (12)$$

To avoid using $\frac{3}{2}$, we can scale up space vectors by $k = \sqrt{\frac{3}{2}}$. This type of scaling up is used in the Park's transformation of Bergen's book [2]. Note the Park's transformation in [2] is defined as follows.

$$\begin{bmatrix} i_0 \\ i_d \\ i_q \end{bmatrix} = \sqrt{\frac{2}{3}} \begin{bmatrix} \frac{1}{\sqrt{2}} & \frac{1}{\sqrt{2}} & \frac{1}{\sqrt{2}} \\ \cos(\theta) & \cos\left(\theta - \frac{2\pi}{3}\right) & \cos\left(\theta + \frac{2\pi}{3}\right) \\ \sin(\theta) & \sin\left(\theta - \frac{2\pi}{3}\right) & \sin\left(\theta + \frac{2\pi}{3}\right) \end{bmatrix} \begin{bmatrix} i_a \\ i_b \\ i_c \end{bmatrix}$$

where θ is the angle the dq reference frame is ahead of the static reference frame.

The relationship of flux linkages, dq currents and excitation current i_F is as follows. Notations of this paper follows the classic text [2].

$$\lambda_F = L_d i_d + k M_F i_F \quad (13)$$

$$\lambda_d = k M_F i_F + L_F i_F \quad (14)$$

$$\lambda_q = L_q i_q \quad (15)$$

B. Faraday's Law

In this subsection, we will express stator and rotor voltage/current relationship applying Faraday's Law.

For the stator voltage, considering the stator resistance r_s, its relationship with the stator current and stator flux linkage is as follow.

$$\overrightarrow{v_s}(t) = -r_s \overrightarrow{i_s}(t) - \frac{d\overrightarrow{\lambda}(t)}{dt} \quad (16)$$

The space vectors will be viewed based on the rotor frame, then the rotating speed of the space vectors will be reduced by ω_m since the rotor speed is ω_m.

$$\overline{v_{dq}} = \overrightarrow{v_s} e^{-j(\omega_m t + \theta_0)} \quad (17)$$

$$\overline{v_{dq}} = -r_s \overline{i_{dq}} - \frac{d\overline{\lambda_{dq}}}{dt} - j\omega_m \overline{\lambda_{dq}} \quad (18)$$

where $\overrightarrow{f_{dq}} = f_d - j f_q$. The dq stator circuits voltage, current an flux linkage relationship is expressed as

$$v_d = -r_s i_d - \frac{d\lambda_d}{dt} - \omega_m \lambda_q \quad (19)$$

$$v_q = -r_s i_q - \frac{d\lambda_q}{dt} + \omega_m \lambda_d. \quad (20)$$

For the EMF induced in the rotor windings, the related equation is

$$0 = -r_F i_F - \frac{d\lambda_F(t)}{dt} \tag{21}$$

In term of fluxes, rotor and stator circuit voltages can be shown as

$$\begin{bmatrix} 0 \\ v_{sd} \\ v_{sq} \end{bmatrix} = - \begin{bmatrix} \frac{L_d r_F}{L_d L_F - kM_F^2} & \frac{-kM_F r_F}{L_d L_F - kM_F^2} & 0 \\ \frac{-kM_F r_s}{L_d L_F - kM_F^2} & \frac{L_F r_s}{L_d L_F - kM_F^2} & \omega_m \\ 0 & -\omega_m & \frac{r_s}{L_q} \end{bmatrix} \begin{bmatrix} \lambda_F \\ \lambda_d \\ \lambda_q \end{bmatrix} - \frac{d}{dt} \begin{bmatrix} \lambda_F \\ \lambda_d \\ \lambda_q \end{bmatrix} \tag{22}$$

The machine speed is related to the net torque.

$$J\frac{d\omega_m}{dt} = T_m - T_e \tag{23}$$

where T_e is the electromagnetic torque and T_m is the mechanical torque. In this study, $T_m = 0$.

The electromagnetic torque T_e is expressed by flux linkages only as follow.

$$T_e = \frac{P}{2}\left[\frac{\lambda_d\lambda_q}{L_q} + \frac{kM_F\lambda_F\lambda_q}{L_dL_F - (kM_F)^2} - \frac{L_F\lambda_d\lambda_q}{L_dL_F - (kM_F)^2}\right] \tag{24}$$

where P is the number of pole pairs.

III. Simulation

For a synchronous machine that operates as an induction machine, free acceleration simulation is made. For this operation, parameters from Table I are used. Equations (22) and (24) are modelled via MATLAB/Simulink. Fig. 2 is the block diagram of the simulated system and Fig. 3 is the Simulnk screen copy. Related to this simulation, three different case studies are analysed.

In the first case, there is no exterior resistances connected to machine for excitation. In the second case, the excitation circuit resistance is 81 times of the original one. In the last case, the resistance is 83 times of the original one.

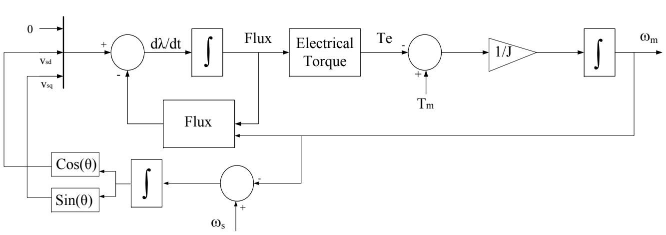

Fig. 2: Block Model of the synchronous machine.

As it is seen $0, v_d, v_q$ are input variables of the synchronous machine. v_d, v_q are computed based on the following equations.

$$v_d = V_m \cos(\omega_s - \omega_m)t \tag{25}$$

$$v_q = -V_m \sin(\omega_s - \omega_m)t \tag{26}$$

where V_m is the voltage magnitude.

TABLE I: Parameters

Nominal voltage	1
ω_s	314 rad/sec
r_s	0.002
r_F	0.00133
L_d	0.00398
L_q	0.00345
L_F	0.00265
kM_F	0.00238
J	0.0000029
P (poles)	2
N	1

A. Case Study I

Machine acceleration is analyzed while there is no exterior excitation effect on it. Electrical torque T_e and angular speed relation is given in Fig. 5 and $\lambda_F, \lambda_d, \lambda_q$ fluxes are presented Fig. 4.

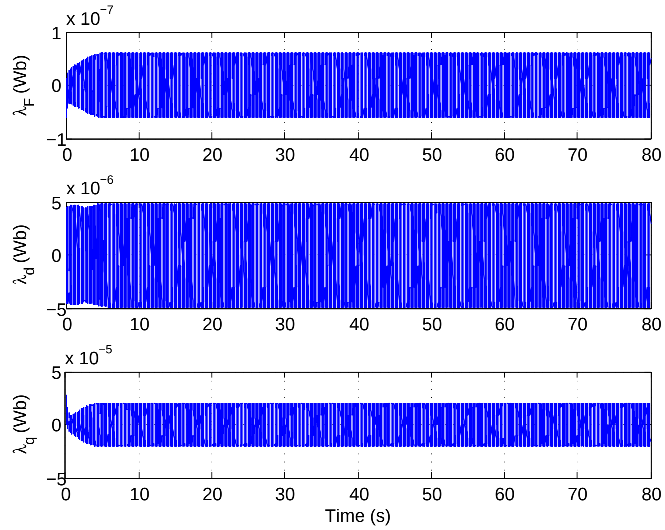

Fig. 4: $\lambda_F, \lambda_d, \lambda_q$.

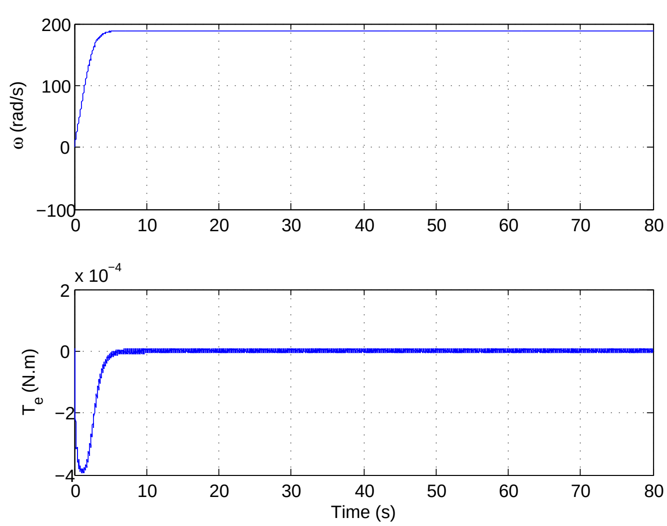

Fig. 5: Filtered T_e and the angular speed.

For this case, angular speed can only reach half of the full.

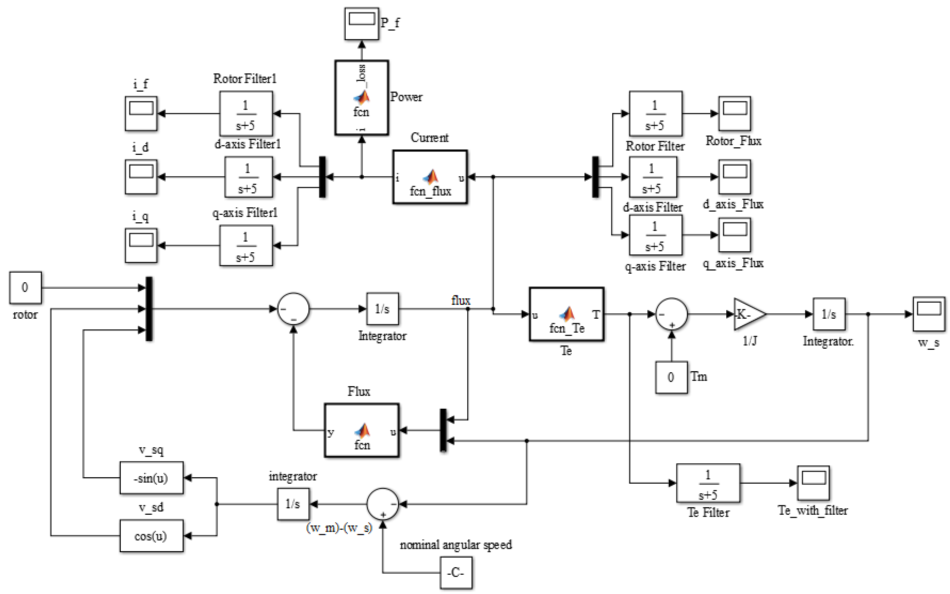

Fig. 3: Block Model of the synchronous machine.

B. Case Study II

It is seen that in the previous case, the machine could not be accelerated to a full speed. In this case, exterior resistance is used which is 81 times of r_F. It can be observed that the angular speed ω_m saturates at 225 rad/sec as shown in Fig. 7.

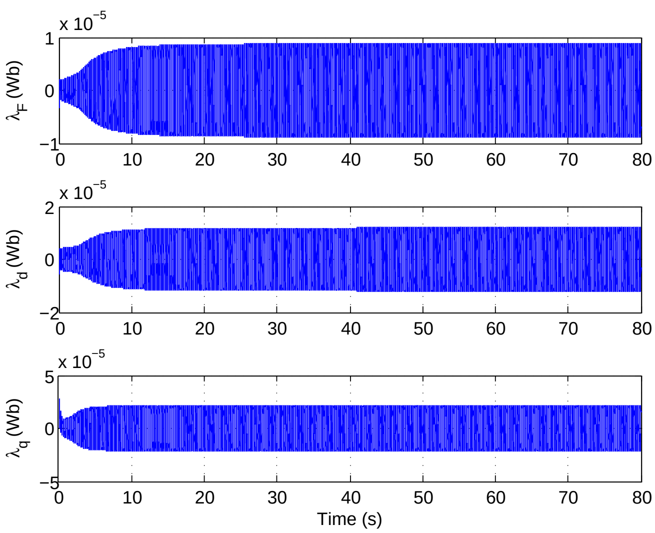

Fig. 6: $\lambda_F, \lambda_d, \lambda_q$.

Fig. 6 presents flux linkages. It is observed that the average flux values are zero at steady-state.

C. Case Study III

For acceleration of the synchronous machine, in this case an exterior resistance is connected to the machine whose value is larger than the previous cases and 83 times of the original rotor resistance. In this way, the machine can accelerate to a full speed as shown in Fig. 9. After a steady speed at about 225 rad/s from 10-25 seconds, the speed quickly accelerates to 377 rad/s. After a dip at 25-30 seconds, the electrical torque T_e saturates and its average value becomes zero. The flux distribution is shown in Fig. 8.

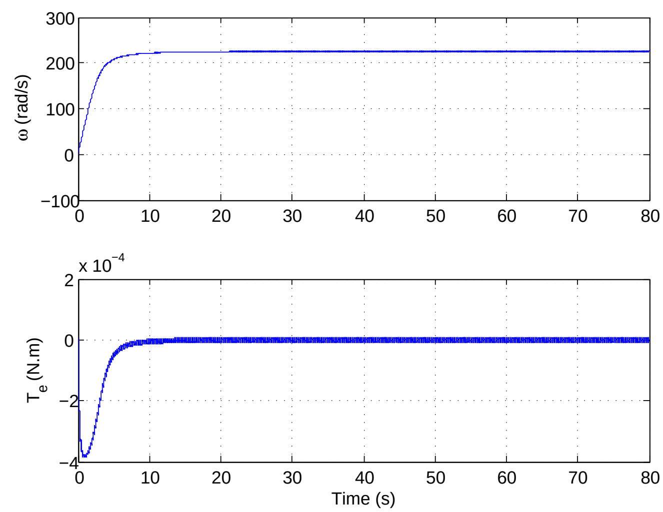

Fig. 7: Speed and filtered T_e.

In this case, angular speed saturates at 377 rad/sec while T_e has stable distribution.

IV. Conclusion

Space vector and two-axis theory are applied to model a three-phase synchronous machine modeling for free acceleration. The dynamic model is derived and built in MATLAB/Simulink. Case studies demonstrate that the model can reasonably represents the free acceleration for a synchronous generator. In lab experiments, external rotor windings are applied while the excitation voltage is short cut for a synchronous machine to start up. This simulation model can accurately model the phenomenon.

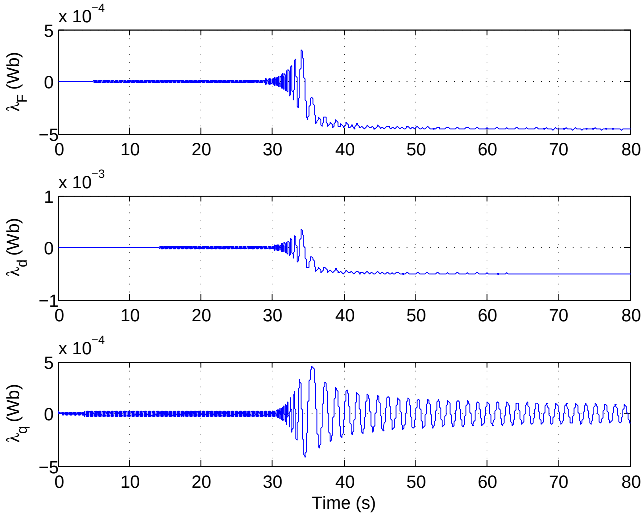

Fig. 8: $\lambda_F, \lambda_d, \lambda_q$.

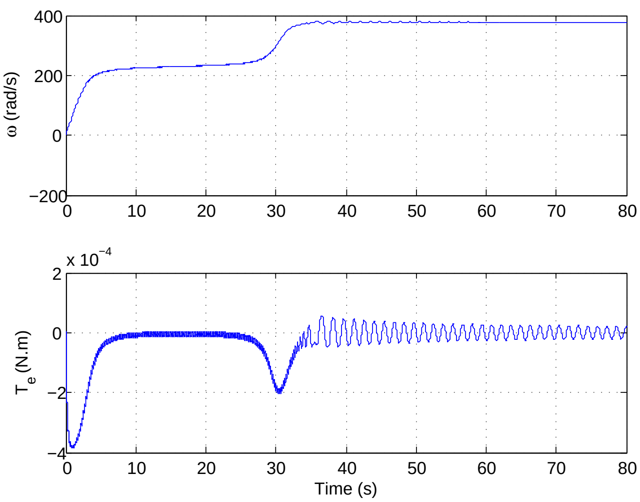

Fig. 9: Speed and filtered T_e.

References

[1] P. C. Krause, O. Wasynczuk, S. D. Sudhoff, and S. Pekarek, *Analysis of electric machinery and drive systems*. John Wiley & Sons, 2013, vol. 75.

[2] A. R. Bergen and V. Vittal, *Power systems analysis*. Prentice Hall, 1999.